

DDFI: Diverse and Distribution-aware Missing Feature Imputation via Two-step Reconstruction

Yifan Song*

HKUST(GZ)

ysong853@connect.hkust-gz.edu.cn

Fenglin Yu*

Carnegie Mellon University

mikukuovo@gmail.com

Yihong Luo*

HKUST

yluocg@connect.ust.hk

Xingjian Tao

HKUST(GZ)

mikukuovo@gmail.com

Siya Qiu

HKUST

squial@connect.ust.hk

Kai Han

Shanghai University of Finance and

Economics

hankai@mail.shufe.edu.cn

Jing Tang

HKUST(GZ) & HKUST

jingtang@ust.hk

Abstract

Incomplete node features are ubiquitous in real-world scenarios, e.g., the attributes of web users may be partly private, which causes the performance of *Graph Neural Networks* (GNNs) to decline significantly. *Feature propagation* (FP) is a well-known method that performs well for imputation of missing node features on graphs, but it still has the following three issues: 1) it struggles with graphs that are not fully connected, 2) imputed features face the over-smoothing problem, and 3) FP is tailored for transductive tasks, overlooking the feature distribution shift in inductive tasks. To address these challenges, we introduce DDFI, a Diverse and Distribution-aware Missing Feature Imputation method that combines feature propagation with a graph-based *Masked AutoEncoder* (MAE) in a nontrivial manner. It first designs a simple yet effective algorithm, namely *Co-Label Linking* (CLL), that randomly connects nodes in the training set with the same label to enhance the performance on graphs with numerous connected components. Then we develop a novel two-step representation generation process at the inference stage. Specifically, instead of directly using FP-imputed features as input during inference, DDFI further reconstructs the features through the whole MAE to reduce feature distribution shift in the inductive tasks and enhance the diversity of node features. Meanwhile, since existing feature imputation methods for graphs only evaluate by simulating the missing datasets with manually masking the features, we collect a new dataset called *Sailing* from the records of voyages that contains naturally missing features to help better evaluate the effectiveness. Extensive experiments conducted on six public datasets and *Sailing* show that DDFI outperforms the

state-of-the-art methods under both transductive and inductive settings.

CCS Concepts

• **Information systems** → **Data mining**; • **Computing methodologies** → **Machine learning algorithms**.

Keywords

Incomplete Graphs, Feature Propagation, Masked Autoencoder

ACM Reference Format:

Yifan Song, Fenglin Yu, Yihong Luo, Xingjian Tao, Siya Qiu, Kai Han, and Jing Tang. 2025. DDFI: Diverse and Distribution-aware Missing Feature Imputation via Two-step Reconstruction. In *Proceedings of The Web Conference (WWW'26)*. ACM, New York, NY, USA, 10 pages. <https://doi.org/XXXXXXX.XXXXXXX>

1 Introduction

Graphs are important structures in the real world, which is capable of modeling complex interactions among various objects. *Graph neural networks* (GNNs) [2, 5, 10, 13, 16, 18, 31] have demonstrated impressive effectiveness in a wide range of applications for graph analysis, including trajectory prediction [21, 23] and user classification [18, 33–35]. Usually, GNNs aggregate node features from neighbors to generate representations that integrate both structure and feature information. Nevertheless, node features often remain incomplete in real-world scenarios. A prominent example arises in the domain of maritime navigation, where critical features such as vessel velocity and wind conditions may be incomplete or missing due to signal interference or sensor limitations. The performance of GNNs will greatly decline due to the incompleteness of node features [25, 28], highlighting the necessity of GNNs with missing node features.

Recently, several methods [14, 15, 25, 27] have been proposed to address the challenge of incomplete node features. Among them, feature propagation (FP) [25] has achieved great success and stands

*These authors contributed equally to this research.

Permission to make digital or hard copies of all or part of this work for personal or classroom use is granted without fee provided that copies are not made or distributed for profit or commercial advantage and that copies bear this notice and the full citation on the first page. Copyrights for components of this work owned by others than the author(s) must be honored. Abstracting with credit is permitted. To copy otherwise, or republish, to post on servers or to redistribute to lists, requires prior specific permission and/or a fee. Request permissions from permissions@acm.org.
WWW'26, April 13–17, Dubai, United Arab Emirates

© 2025 Copyright held by the owner/author(s). Publication rights licensed to ACM.
ACM ISBN 978-1-4503-XXXX-X/18/06
<https://doi.org/XXXXXXX.XXXXXXX>

*These authors are co-first authors.

out as a representative method, which utilizes the normalized adjacency matrix for iterative feature propagation and resets known features to their original values after each iteration.

However, node feature imputation methods based on FP face three fundamental challenges. **Firstly**, the quality of features imputed by FP heavily relies on the connectivity of graphs. As shown in Figure 1a, where FP-LCC means applying FP on the largest connected component of the dataset, the performance will drop observably when facing graphs with multiple connected components. **Secondly**, FP faces the over-smoothing problem in transductive tasks. Figure 1b gives the MAD metric [3] of the features generated by FP, a widely used metric to quantify over-smoothing. It could be seen that FP yields a MAD below 0.4, indicating that FP limits the diversity of node features. **Moreover**, employing FP in inductive tasks can result in feature distribution shift during the inference stage, thus damaging the performance under different downstream tasks. Specifically, as shown in Figure 2, only partial graph structure is available during training in inductive tasks, while features are propagated over the entire graph in the inference stage. Since FP relies on graph structure to impute the features, the distribution of imputed features during training differs from that during inference, resulting in the feature distribution shift.

To tackle these problems, we propose the Diverse and Distribution-aware Missing Feature Imputation (**DDFI**) that utilizes the FP to generate the initial imputed feature and then designs a two-step reconstruction with MAE model to improve the diversity of representation and reduce the feature distribution shift. It first devises a simple yet effective technique called Co-Label Linking (CLL) to reduce the number of connected components, which randomly connects the nodes in the training set with the same label to reduce the number of connected components without damaging the homophily of the graphs. Then, inspired by GraphMAE [9], we utilize a graph-based MAE model to learn the feature distribution during the training stage. It learns the encoder by masking features with our strategy based on Gaussian distribution and forcing the model to reconstruct them, which could improve the diversity of representation. Concurrently, we design a novel two-step inference for DDFI to reduce the feature distribution shift in the inductive tasks. During inference, it first reconstructs the FP-imputed features using the full encoder-decoder and then passes these features through the encoder again to obtain final representations. The two-step process leverages the autoencoder’s ability to align feature distributions between training and inference, reducing feature distribution shift and improving the performance of inductive tasks.

Furthermore, existing methods for feature imputation often mask features in datasets with artificially generated missing patterns to simulate scenarios of missing data, which does not reflect the natural occurrence of incomplete features in real-world settings. To help better evaluate the effectiveness of feature imputation methods under naturally missing conditions, we propose a new dataset called **Sailing**, which extracts a portion of real maritime data provided by the Danish Maritime Authority (DMA) [1]. Notably, 80.4% of the features in this dataset are missing naturally, without artificial intervention. To our best knowledge, we are the first to propose a real-world dataset with naturally missing features, which can better verify the effectiveness of missing feature imputation methods in real scenarios.

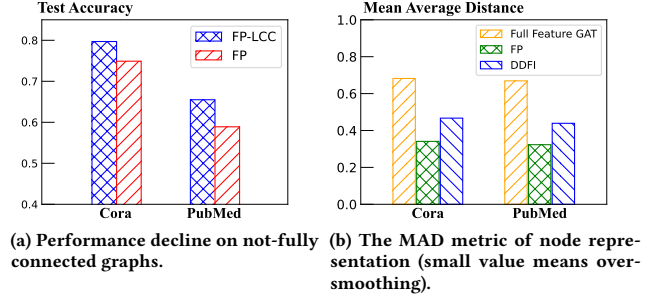


Figure 1: The analysis on the challenges of FP-based methods.

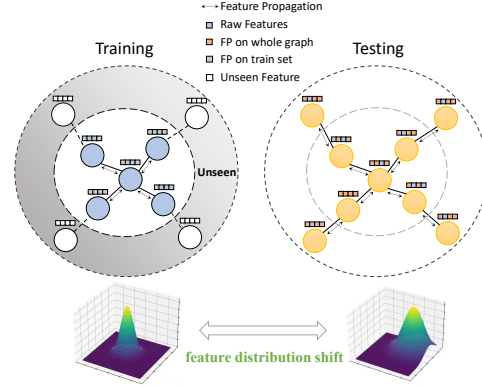


Figure 2: The problem of FP on inductive tasks.

In summary, our main contributions are listed as follow:

- We design a simple yet effective algorithm called CLL to enhance the performance of feature imputation for not fully connected graphs.
- We propose the DDFI model, which enhances the feature imputation by a graph-based MAE model with a novel two-step inference to improve the diversity of generated features and address the feature distribution shift under inductive tasks.
- Extensive experiments conducted on seven datasets including a newly collected dataset called Sailing show that DDFI outperforms all the baselines in node classification and link prediction.

The remainder of this paper is organized as follows. In Section 2, we give notations and the necessary preliminary knowledge. In Section 3, we present our approach DDFI by providing an in-depth discussion of motivations as well as the details of model design. The results of experiments on node classification and link prediction are reported in Section 4. In Section 5, we discuss related works and contrast them with ours. Finally, we conclude our work and discuss some future directions in Section 6.

2 Preliminaries

2.1 Notations

For an undirected graph $G = (V, E)$, let $A \in \mathbb{R}^{n \times n}$ be the adjacency matrix and $Y \in \mathbb{R}^{n \times 1}$ be the label vector, where y_i represents the label of node v_i . For a node feature matrix with missing values,

represented as $\mathbf{X} \in \mathbb{R}^{n \times d}$, graph learning with missing features aims to find a function L that satisfies $f(L(\mathbf{X}), \mathbf{A}) \approx \mathbf{Y}$, where the function L is a missing feature imputation algorithm, and f can use GNN or MLP to map the feature to the label. We denote \mathbf{A}_{tr} and \mathbf{X}_{tr} as the adjacency matrix and feature matrix during training stage, respectively, where $\mathbf{A}_{tr} = \mathbf{A}$ and $\mathbf{X}_{tr} = \mathbf{X}$ for transductive tasks.

2.2 Feature Propagation

Feature Propagation (FP) algorithm [25] imputes missing node features based on the minimization of the Dirichlet energy. It iteratively diffuses features across the given graph G , the entire process is shown in Algorithm 1. FP can be combined with any GNN model to solve downstream tasks, outperforming former proposed methods for incomplete graph with missing features by a significant margin. However, as stated in Section 1, FP needs to propagate the features of the entire graph again at the inference stage for inductive tasks, which leads to a feature distribution shift problem that can cause FP to perform poorly on inductive inference. We will discuss in Section 3 how DDFI utilizes training GraphMAE and two-step inference to enhance missing feature imputation on inductive tasks.

Algorithm 1: Feature Propagation [25]

Input: Initial feature vector \mathbf{x} (with missing values),
Adjacency matrix \mathbf{A} .

Output: Reconstructed feature vector \mathbf{x} .

$\mathbf{y}_k \leftarrow \mathbf{x}_k$;

$\tilde{\mathbf{A}} \leftarrow \mathbf{D}^{-\frac{1}{2}} \mathbf{A} \mathbf{D}^{-\frac{1}{2}}$;

while \mathbf{x} has not converged **do**

$\mathbf{x} \leftarrow \tilde{\mathbf{A}} \mathbf{x}$;

$\mathbf{x}_k \leftarrow \mathbf{y}_k$;

 // Reset known features

return \mathbf{x} ;

2.3 Analysis of Feature Distribution Shift

In this section, we provide a theoretical formulation about the feature distribution shift issue. If we hypothesize that $L(\mathbf{X}, \mathbf{A})$ denotes the representation generated by the FP-based imputed feature matrix and GNN, with \mathbf{X} as the feature matrix and \mathbf{A} as the adjacency matrix, $D(L(\mathbf{X}, \mathbf{A}))$ denotes a two-dimensional discrete distribution derived from the matrix $L(\mathbf{X}, \mathbf{A})$. \mathbf{A}_{tr} and \mathbf{X}_{tr} are the adjacency matrix and the feature matrix of the training graph, respectively. The feature shift between the training and testing stages in inductive tasks can be written as follows:

$$\Delta = \mathcal{F}(D(L(\mathbf{X}, \mathbf{A})), D(L(\mathbf{X}_{tr}, \mathbf{A}_{tr})))$$

, where \mathcal{F} is an optional function that measures the difference in distribution.

According to the above formulation, the core reason behind the feature distribution shift issue is that **the distribution of feature imputed by feature propagation strictly rely on the graph structure**, make the difference between training and inference.

Algorithm 2: Co-label Linking

Input: Graph $\mathcal{G} = (\mathcal{V}, \mathcal{E})$, Features \mathbf{X} , Labels \mathbf{y} , Parameters
 k, τ , Candidate size M .

Output: Graph $\tilde{\mathcal{G}} = (\mathcal{V}, \tilde{\mathcal{E}})$.

$\tilde{\mathcal{E}} \leftarrow \mathcal{E}$;

foreach node $v_i \in \mathcal{V}$ **do**

 // Sample candidate set

 Sample a candidate set $C_i \subset \mathcal{V} \setminus \{v_i\}$ of size M ;

 // Compute distribution

foreach $v_j \in C_i$ **do**

$w_j \leftarrow \text{sim}(\mathbf{x}_i, \mathbf{x}_j)$;

 // Normalization

$Z \leftarrow \sum_{v_j \in C_i} \exp(w_j/\tau)$;

foreach $v_j \in C_i$ **do**

$p_j \leftarrow \exp(w_j/\tau)/Z$;

 // Sample from candidates and link

 Sample a set S_i of k nodes from C_i using $\{p_j\}$;

$\mathcal{V}_{\text{link}} \leftarrow \{v_j \in S_i \mid y_j = y_i\}$;

$\tilde{\mathcal{E}} \leftarrow \tilde{\mathcal{E}} \cup (\{v_i\} \times \mathcal{V}_{\text{link}})$;

return $(\mathcal{V}, \tilde{\mathcal{E}})$;

3 The Framework of DDFI

In this section, we present the complete workflow of DDFI. Firstly, we introduce a simple yet effective algorithm called Co-Label Linking (CLL), designed to enhance the effectiveness of feature propagation by addressing challenges arising from disconnected graphs. Secondly, DDFI leverages the graph-based MAE model trained on feature-propagated graphs to generate representations with higher diversity than FP for downstream tasks. Unlike a naive combination of feature propagation and MAE, which lacks robustness on incomplete graphs, DDFI incorporates a Gaussian distribution-based feature masking strategy during training. Also, to increase the diversity of imputed features and alleviate the feature distribution shift problem in inductive tasks, DDFI employs a two-step inference process that reconstructs the imputed feature through the whole encoder-decoder structure. The overall workflow is illustrated in Figure 3.

3.1 Co-label Linking

In this part, we present how to enhance the performance of feature propagation for missing node features imputation through a simple but effective way. To reduce the connected components of the graph, a naive way is to randomly link node pairs between each connected component. Although this approach can remit the disconnectivity of the graphs, it can reduce the homophily of the graphs, which will also damage the performance of FP [25]. To avoid reducing the homophily, we propose an algorithm called Co-Label Linking (CLL). Specifically, for each node v_i , CLL will randomly choose k nodes and add edges between nodes with the same label of v_i . The Algorithm 2 shows the entire CLL process.

It is evident that after applying CLL, the homophily index of the new graph \tilde{G} is at least as high as the original graph G . Using

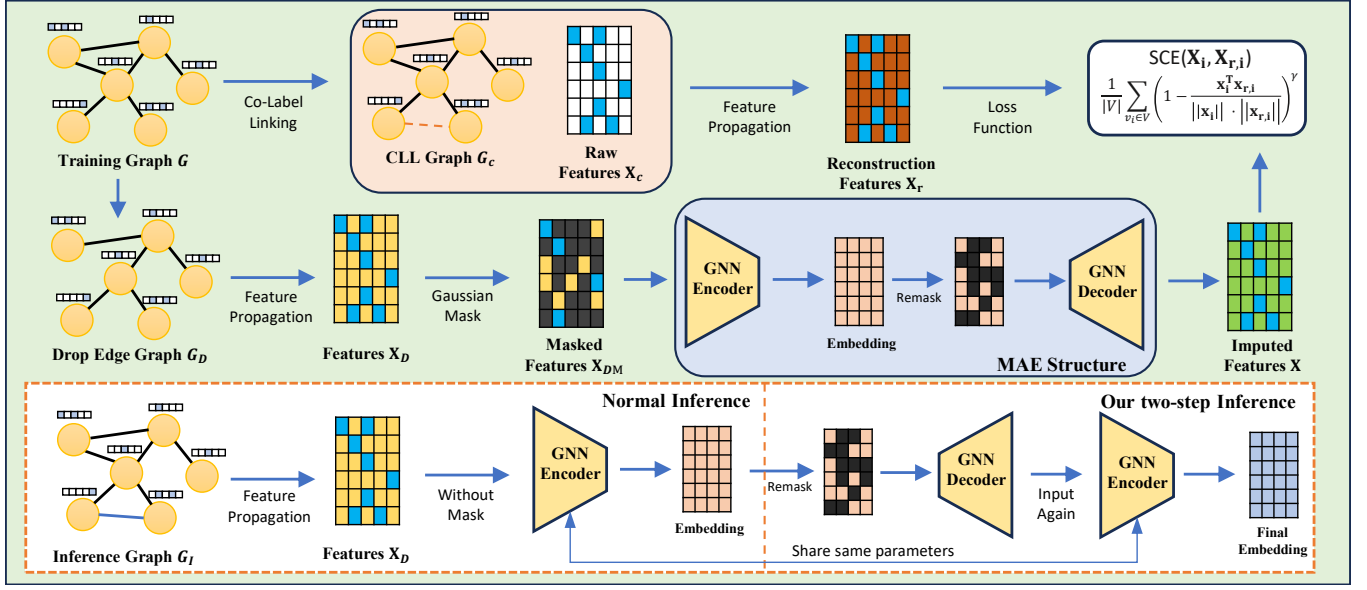


Figure 3: Training and inference process of DDFI.

CLL, we can reduce the number of connected components in the graph without decreasing its homophily, thereby improving the performance of FP complement features.

3.2 Model Training and Two-Step Inference

3.2.1 Motivation Analysis. As stated in Section 1, when facing the inductive tasks where the graph structure is different between training and inference, the features imputed on the training set will have a significantly different distribution from the features imputed on the full graph structure at inference stage. More precisely, for the transductive tasks, the graph structure seen in the training set is the same as in the test set (i.e., $\mathbf{A}_{tr} = \mathbf{A}$), so the features added during training and inference are also the same (i.e., $\tilde{\mathbf{X}}_{tr} = \tilde{\mathbf{X}}$). For the inductive tasks, since the whole graph structure has changed at inference stage, the feature propagation needs to be performed on the new full graph \mathbf{A} to obtain the new imputation feature $\tilde{\mathbf{X}}$. In this case, the change in the graph structure will result in a different distribution of imputation features while the GNN model for downstream tasks is trained based on $\tilde{\mathbf{X}}_{tr}$. The distribution shift of the imputed features on test set will seriously degrade the performance of the FP-based framework on inductive tasks.

In fact, designing a model that can adapt to both graph structure changes and different feature distributions to ensure the performance of inductive tasks is very difficult. To solve the missing feature imputation problem in the inductive setting, it is more important to keep the consistency of feature distribution between training and inference, rather than modifying the feature distribution consistent with the graph structure change. The motivation behind this is that most GNN models have inherent inductive learning ability for graph structures (i.e., graph structure changes do not significantly reduce performance) [8, 22, 30]. Based on this consideration, we design the two-step inference, which reconstructs the propagated features through the entire encoder-decoder structure

to keep them similar to the training feature distribution at the inference stage. The details of the training and inference processes will be provided below.

3.2.2 Training Stage. As mentioned above, we hope to reduce the feature distribution shift by reconstructing features using graph-based MAE model. Nevertheless, general MAE model trains by minimizing the difference between the reconstructed features and the input, which is not robust for missing feature imputation since the proportion of known features is low in graphs with missing features and the imputed features by FP have much noise. To solve this issue, DDFI will obtain feature inputs from the encoder-decoder structure by propagating features on randomly dropped edges in the graph, and then the final reconstructed result will have the smallest difference with the features obtained by propagating features on the graph after CLL. By distinguishing between the input of the MAE model and the reconstruction target, DDFI can effectively enhance its generalization performance and robustness. Concretely speaking, DDFI will obtain the model input for each epoch as follows:

$$\mathbf{A}_{D,i} = \text{Drop}(\mathbf{A}_{tr}), \quad \mathbf{X}_{D,i} = \text{FP}(\mathbf{X}_{tr}, \mathbf{A}_{D,i}), \quad (1)$$

where $\mathbf{A}_{D,i}$ is the structure of graph in i -th epoch after randomly dropping edges, FP is the feature propagation function and $\mathbf{X}_{D,i}$ is the input feature of MAE model in i -th epoch.

To enhance the sensitivity to each feature dimension in the reconstruction process, we apply a masking strategy based on a Gaussian distribution to the input features as follows:

$$\mathbf{W} \sim \mathcal{N}(0, 1), \quad \mathbf{X}_{DM,i} = \mathbf{X}_{D,i} \odot \sigma(\mathbf{W} + \text{offset}), \quad (2)$$

where $\mathcal{N}(0, 1)$ is a normally distributed Gaussian noise, and the offset is calculated as $\log\left(\frac{\text{mask rate}}{1 - \text{mask rate}}\right)$. The probability of masking is given by $\sigma(\mathcal{N}(0, 1) + \text{offset})$, where σ denotes the sigmoid function. We then use this distribution to generate masks via a Bernoulli distribution, thus it can randomly mask different dimensions of node feature to improve the sensitivity of DDFI.

Next, DDFI will perform feature propagation on the graph after CLL to obtain the feature matrix \mathbf{X}_r as the complete reconstruction view. We will train the MAE model using the SCE loss function as follow:

$$L = \frac{1}{|V|} \sum_{v_i \in V} \left(1 - \frac{\tilde{\mathbf{x}}_i^\top \mathbf{x}_{r,i}}{\|\tilde{\mathbf{x}}_i\| \cdot \|\mathbf{x}_{r,i}\|}\right)^\gamma, \quad (3)$$

where $\tilde{\mathbf{x}}_i$ is the output feature of node v_i after the MAE structure, $\mathbf{x}_{r,i}$ is the feature of node v_i under reconstruction view, γ is a hyper-parameter. Through filling the gap between the output of GraphMAE and reconstruction feature, DDFI could force the model to learn how to reconstruct the feature distribution and reduce the noise in the original feature.

3.2.3 Inference Stage. For inference stage, DDFI can be represented as follow:

$$\begin{aligned} \text{Step 1: } \mathbf{X}_r &= \text{Decoder}(\text{Encoder}(\text{FP}(\mathbf{X}, \mathbf{A}))), \\ \text{Step 2: } \mathbf{Z} &= \text{Encoder}(\mathbf{X}_r), \end{aligned} \quad (4)$$

where Encoder and Decoder are two GNN models. Different from the normal MAE, which uses the output of encoder as the embedding for downstream tasks, DDFI adopts a two-step inference. Firstly, the feature after propagation will be reconstructed through the whole encoder-decoder model. This step takes advantage of the property that MAE is able to learn the feature distribution in the training stage, which could reduce feature distribution shift in the reconstruction process. It alleviates the difficulty of the basic FP model in the face of inductive tasks. Then we send it into a GNN encoder that shares the same parameters with the trained encoder in the MAE model to get the final embedding applying for different downstream tasks.

In summary, DDFI introduces the concept of CLL to reduce the connected component. In addressing the over-smoothing problem and feature distribution shift, it leverages a graph-based MAE model for feature reconstruction, which adopts a two-step reconstruction process during inference. Also, we utilize edge dropping and Gaussian masking to improve the robustness of DDFI. Through these strategies, it demonstrates strong performance in both transductive and inductive tasks, which overcomes the challenges of existing feature imputation methods.

4 Experiments

In this section, we evaluate DDFI compared with six baselines across two tasks: node classification and link prediction. For node classification, we conduct experiments under both transductive and inductive settings. For link prediction, we evaluate all the methods as specifically demonstrated in Section 4.4. We also conduct ablation study and show the visualization results in Section 4.5 and 4.6. Due to the page limit, the results of parameter sensitivity analysis can be found in the Appendix A.4. The experiments are conducted on a single machine with an Intel Xeon 8377C CPU, an Nvidia 3090 GPU (24GB), and 1TB of RAM.

4.1 Datasets and Baselines

To verify the effectiveness of DDFI in real-world scenarios, we first propose a new dataset for missing feature imputation called **Sailing**, which is collected from Danish Nautical Data Records [1]. We select a subset from the original data and construct the graph

Table 1: Dataset statistics (D: Graph Density, C: Clustering coefficient).

Dataset	Nodes	Edges	D (10^{-3})	C
Cora	2,708	10,566	1.48	0.261
Citeseer	3,327	9,228	0.85	0.141
PubMed	19,717	88,651	0.22	0.060
Ogbn-Arxiv	169,343	1,166,243	0.08	0.118
Flickr	89,250	899,756	0.22	0.033
Reddit	232,965	23,213,838	0.42	0.240
Sailing	5,014	55,458	2.21	0.323

by dividing the grid according to latitude and longitude. Trajectory points in the same grid or adjacent grids are connected as edges according to a certain probability distribution. Appendix A.1 reports more construction details. After the construction, the Sailing dataset naturally has 80.4% missing features, providing a new benchmark dataset for missing feature imputation methods to validate their effectiveness in real-world scenarios. Next, we evaluate the transductive node classification task on five datasets: Cora, Citeseer, PubMed, Ogbn-Arxiv and Sailing. To validate our effectiveness on inductive tasks, we evaluate the inductive node classification task on three datasets: Reddit, Flickr and Sailing. The dataset statistics are shown in Table 1.

DDFI is compared with seven baselines, including: (1) two standard graph embedding methods: GCN [20] and GAT [31]; and (2) five methods designed for missing feature scenarios: GCNMF [27], PaGNN [15], FP [25], ASD-VAE [17] and PCFI [28]. Following previous work [25], we generate the missing features with uniform and structural types as input for all feature imputation the methods, where uniform missing means that each feature dimension of each node is missing randomly and structural missing represents either we observe all features for a node, or we observe none. For FP and PCFI, we use the same type of GNN as the encoder in DDFI for a fair comparison.

4.2 Experimental Setup

For the transductive and inductive node classification task, we report the mean and standard error of the test accuracy with running five times. For the link prediction task, AUC and AP scores [6] are used to validate the effectiveness of all the methods following prior work [26, 36, 37]. All results are under 90% missing feature rate (except for Sailing, which naturally has an 80.4% missing feature rate). For DDFI, we first simply set the $\text{sim}(\mathbf{x}_i, \mathbf{x}_j) = 1$, $\tau = 1$ and $M = |V|$ to avoid excessive parameter tuning. Then we adjust other parameters to achieve the best result on the validation set, with all details provided in Appendix A.2. For other baselines, we use their official code to reproduce the results.

4.3 Node Classification

The node classification task involves predicting unknown labels of nodes in a graph. For the transductive setting, the whole graph structure is available and we need to predict the labels of the test set with training labels. Here we use the official split for Cora, Citeseer, PubMed and Ogbn-Arxiv, and split the Sailing with 40%-30%-30%

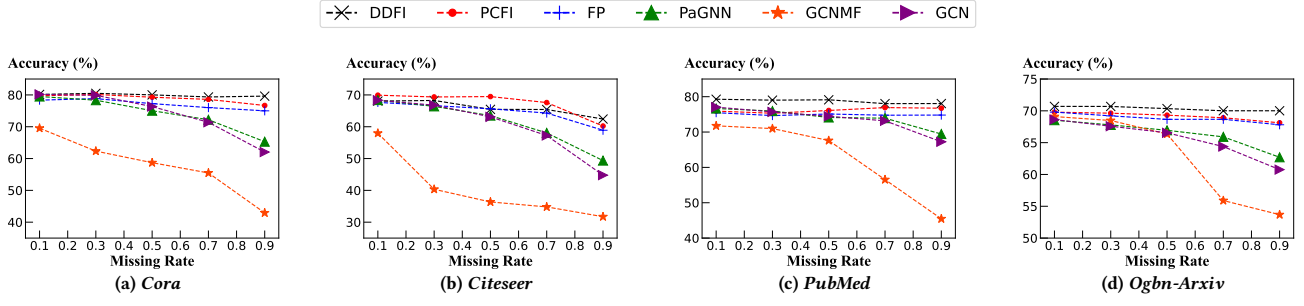


Figure 4: Performance under different missing rates for transductive learning (best viewed in color).

Table 2: Transductive node classification results.

MISSING TYPE	DATASET	GAT	GCN	GCNMF	PAGNN	FP	PCFI	ASD-VAE	DDFI
UNIFORM	CORA	66.06 \pm 1.37	62.02 \pm 0.95	42.94 \pm 2.36	65.30 \pm 1.31	74.98 \pm 0.88	<u>76.68 \pm 1.55</u>	71.93 \pm 0.76	79.62 \pm 0.39
	CITSEER	47.68 \pm 1.30	44.78 \pm 2.09	30.14 \pm 4.68	49.36 \pm 1.78	58.90 \pm 1.00	<u>60.22 \pm 0.80</u>	56.93 \pm 0.94	62.90 \pm 0.62
	PUBMED	67.38 \pm 1.24	67.24 \pm 1.84	45.00 \pm 3.04	69.44 \pm 1.01	75.80 \pm 0.62	<u>76.74 \pm 0.47</u>	OOM	78.56 \pm 0.56
	OGBN-ARXIV	58.74 \pm 0.21	60.76 \pm 0.28	57.36 \pm 0.74	62.49 \pm 0.20	67.84 \pm 0.40	<u>68.27 \pm 0.18</u>	OOM	69.54 \pm 0.26
STRUCTURAL	CORA	54.88 \pm 1.43	53.18 \pm 2.19	24.80 \pm 6.72	55.26 \pm 2.31	73.06 \pm 1.86	<u>73.98 \pm 1.61</u>	70.99 \pm 1.01	77.44 \pm 1.04
	CITSEER	40.52 \pm 1.90	37.30 \pm 1.95	20.02 \pm 2.53	40.34 \pm 2.26	55.44 \pm 1.44	<u>59.38 \pm 1.02</u>	54.52 \pm 1.39	60.04 \pm 0.46
	PUBMED	63.28 \pm 1.48	62.10 \pm 2.00	40.46 \pm 4.15	64.74 \pm 1.09	73.78 \pm 0.35	<u>75.08 \pm 2.40</u>	OOM	77.80 \pm 0.67
	OGBN-ARXIV	60.97 \pm 0.33	56.83 \pm 0.43	34.89 \pm 4.36	60.70 \pm 0.42	<u>67.77 \pm 0.15</u>	67.73 \pm 0.28	OOM	68.15 \pm 0.25
NATURAL	SAILING	63.07 \pm 1.47	64.45 \pm 0.62	48.66 \pm 2.53	67.47 \pm 1.11	66.91 \pm 0.90	<u>68.45 \pm 0.36</u>	66.71 \pm 1.02	70.95 \pm 0.76

for train, validation and test. For the inductive setting, only nodes that appear in the training set are available during training, and the whole graph structure is available for inference. We split the Flickr and Reddit with 20%-40%-40% for train, validation and test, and use the same split as transductive setting for Sailing.

Results. Table 2 reports the results of all the methods on the transductive node classification task with uniform and structural missing types. DDFI outperforms all the baselines across every dataset. Specifically, the improvements on four public datasets with uniformly missing features range from 1.33% to 2.94% compared with PCFI, which has the best performance in missing feature imputation. We also achieve a significant improvement of 2.50% compared with the strongest baseline on Sailing, demonstrating that our method can better handle real-world scenarios. When it comes to structurally missing features, our method still performs well against several baselines, particularly on Cora, where it surpasses PCFI by an accuracy margin of 3.46%.

Based on the analysis of experiments on multiple datasets, methods utilize feature imputation outperform normal GNNs. An exception to this trend is GCNMF, whose performance significantly declines when the proportion of missing features is large. FP performs better in the transductive experiment because it fills in the missing features, whereas methods such as GCN and GAT have much lower performance as they assume the node features are complete. DDFI achieves the best results by utilizing components such as CLL.

Second, we evaluate the performance of all methods under inductive setting. Since ASD-VAE runs out-of-memory on Flickr and

Reddit and it does not design for inductive task, we do not include its result and add GAT into comparison. Table 3 shows the inductive node classification results. For the inductive task, common methods that do not consider the feature distribution shift between training and inference such as FP and PCFI result in poor performance, while other methods based on GNNs also struggle to achieve strong results. DDFI achieves the best results with using masked autoencoders to learn the feature distribution and reconstruct the features. For example, DDFI outperforms PCFI with a significant improvement of 13.56% on Sailing, which validates the effectiveness of our proposed components.

Additionally, we evaluate the performance of all methods across varying missing rates (ranging from 10% to 90%) on four datasets: Cora, Citeseer, Pubmed, and Ogbn-arxiv. The results are shown in Figure 4. It reveals that most methods not based on feature propagation experience a significant performance degradation as the missing rate increases. In contrast, DDFI achieves the best performance across different missing rates on Cora, Pubmed, and Ogbn-arxiv. However, on the Citeseer dataset, PCFI outperforms our method at low missing rates. This can be attributed to the extremely high dimensionality of Citeseer’s features, which aligns well with the multi-channel completion strategy employed by PCFI. Notably, our method still achieves the best performance at a 90% missing rate, underscoring its robustness in handling severe feature sparsity for real-world datasets.

Table 3: Inductive node classification results.

MISSING TYPE	DATASET	GAT	GCN	GCNMF	PAGNN	FP	PCFI	DDFI
UNIFORM	FLICKR	43.90 \pm 0.94	44.99 \pm 0.33	47.73 \pm 2.71	49.46 \pm 0.12	48.10 \pm 0.77	47.72 \pm 0.47	51.97 \pm 0.07
	REDDIT	49.90 \pm 2.50	84.08 \pm 0.85	OOM	86.77 \pm 0.50	86.28 \pm 2.69	OOM	93.95 \pm 0.15
STRUCTURAL	FLICKR	42.48 \pm 0.09	42.78 \pm 0.07	43.09 \pm 1.01	45.72 \pm 0.29	45.94 \pm 1.59	45.25 \pm 0.68	50.52 \pm 0.16
	REDDIT	77.96 \pm 2.68	84.86 \pm 0.97	OOM	90.57 \pm 0.32	89.47 \pm 1.91	OOM	92.27 \pm 0.46
NATURAL	SAILING	59.64 \pm 0.97	61.62 \pm 0.60	45.10 \pm 4.84	64.85 \pm 0.56	63.44 \pm 0.98	63.52 \pm 0.21	77.08 \pm 0.36

4.4 Link Prediction

The link prediction task involves predicting unknown edge labels in graphs. For this task, we conduct experiments using two different feature-missing methods (uniform and structural) on five datasets (Cora, Citeseer, Pubmed, OGBN-Arxiv and Sailing). We sample the positive and negative edges in ratios of 0.05 and 0.1 for validation and test, respectively, for the three benchmark datasets: Cora, Citeseer, and Pubmed. To increase the difficulty of the task for Sailing, we set 60%-10%-30% as the split rates for training, validation and testing respectively. For the validation and test datasets, we simultaneously generate the same number of negative edges randomly sampled from the complement graph. We conducted experiments on four baselines: GCNMF, GNN, FP, and PCFI for comparison. The process can be split into two steps. First, follow previous work [12], we use the edges in the training dataset to complete missing features in the graph. Then, we fit the features to a Graph Autoencoder (GAE) [19] with an output of same dimensions. By using GAE in the package Torch Geometric [7], we ensure fairness among the baselines and our method. The final AUC and AP are used to validate the performance of the models.

Results. Table 4 shows the results of link prediction with different methods for uniform and structural missing features respectively. Also, we provide the results on the Sailing with naturally missing features. In summary, DDFI achieves the best performance across all the datasets. For the four datasets Cora, Citeseer, PubMed and Ogbn-Arxiv, when features are missing uniformly, the AUC improvements on the four public datasets range from 3.16% to 16.82% while the AP improvements ranging from 2.79% to 11.56% compared to the state-of-the-art method, PCFI. For structural missing features, the AUC improvements range from 2.92% to 14.23% while the AP improvements ranging from 2.53% to 10.18%. Through the excellent performance of DDFI for link prediction task under different missing types, it can validate the effectiveness of our proposed method. When we validate the performance on the natural missing dataset Sailing, our model still slightly outperforms several others. This demonstrates that DDFI can effectively handle natural missing features and is more suitable for real-world scenarios.

4.5 Ablation Studies

We conduct several ablation studies to further confirm the effects of the main components in DDFI. We select four public benchmark datasets: Cora and PubMed for the transductive node classification task, Flickr and Reddit for the inductive node classification task. The results are shown in Table 5.

Effect of reconstruction. We investigate the impact of the reconstruction component in the two-step inference process of DDFI

by comparing results with and without it. In the inductive setting, DDFI exhibits a performance decline when the reconstruction component is removed, with accuracy drops ranging from 1.14% to 1.27%. This underscores the importance of reconstruction in aligning feature distributions, as discussed in Section 3. Similarly, in the transductive setting, reconstruction enhances performance, with improvements ranging from 0.82% to 0.98%. We attribute this improvement to the reduction of noise in the features during the reconstruction process. Although the reconstruction is not specifically designed for transductive tasks, we include the reconstruction component as an optional parameter for such tasks.

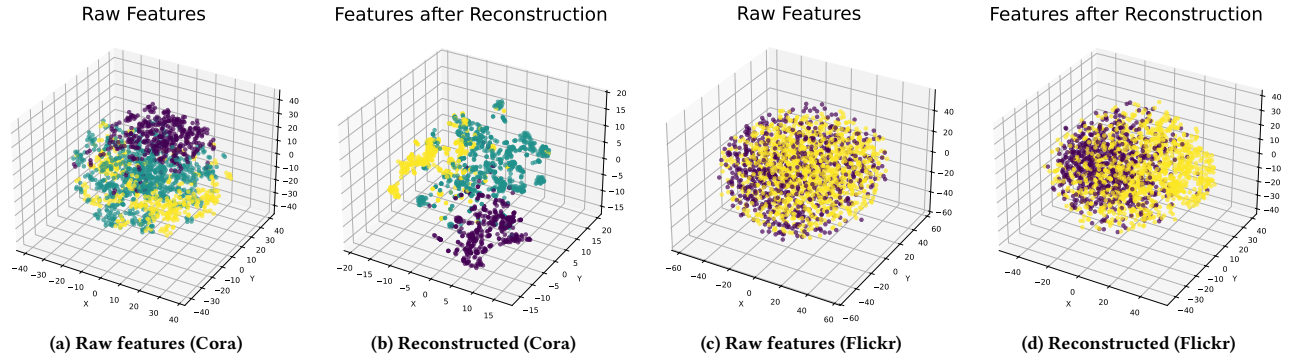
Effect of Co-Label Linking. Co-Label Linking (CLL) can enhance graph homogeneity and reduce the number of isolated components, both of which have been demonstrated to improve performance in graph-related tasks. To validate the effectiveness of CLL, we conduct experiments on specific datasets with and without it. The results show that DDFI experiences a performance decline ranging from 0.58% to 2.52% on the Cora and PubMed datasets when CLL is removed, confirming its effectiveness in transductive tasks. However, the results show a decrease of 0.04% in performance on the Flickr dataset and an increase of 0.01% on the Reddit, indicating that CLL has negligible impact in inductive tasks. This outcome can be attributed to the design of CLL, which primarily reduces the connected components, whereas the key challenge in inductive settings lies in learning feature distribution reconstruction during training and generalizing it to unseen data. Nevertheless, CLL is still potentially valuable as an optional preprocessing module to deal with the more sparsely graphs in inductive task that may arise in the future. Therefore, we keep it as part of the framework.

4.6 Visualization

To demonstrate the effect of feature reconstruction via GraphMAE, we visualize the raw feature distribution and the feature distribution after reconstruction. We use t-SNE [29], a dimensionality reduction technique, to map the data to three dimensions for easier visualization. Figure 5 shows the results for the Cora dataset under the transductive setting, with different node labels shown in different colors. Note that the labels of the test dataset were unknown during model fitting. We find that after reconstruction, different classes are distributed farther apart, while nodes of the same class are located closer together. Additionally, a slightly higher margin between feature nodes with different labels appears, indicating greater robustness for handling downstream tasks. Clearly, the features after reconstruction are better suited for fitting a Linear Classifier for node classification or a GAE for link prediction. This indicates that GraphMAE can strengthen and optimize the missing

Table 4: Link prediction results.

	DATASET	GCNMF		GCN		FP		PCFI		DDFI	
		AUC	AP	AUC	AP	AUC	AP	AUC	AP	AUC	AP
UNIFORM	CORA	61.09 \pm 1.54	61.73 \pm 2.23	71.13 \pm 2.19	72.86 \pm 2.62	86.65 \pm 0.68	89.21 \pm 0.35	86.16 \pm 0.89	88.91 \pm 0.46	94.92 \pm 0.81	94.36 \pm 0.87
	CITSEER	59.00 \pm 1.72	58.54 \pm 2.09	72.31 \pm 2.44	75.65 \pm 2.27	<u>81.18 \pm 1.17</u>	<u>86.02 \pm 1.30</u>	80.68 \pm 1.38	85.44 \pm 1.01	93.69 \pm 1.04	92.91 \pm 0.94
	PUBMED	61.62 \pm 0.51	69.46 \pm 0.67	82.18 \pm 0.77	82.33 \pm 0.45	81.15 \pm 0.19	85.61 \pm 0.19	80.72 \pm 1.02	85.62 \pm 0.56	97.54 \pm 0.27	97.18 \pm 0.27
	OGBN-ARXIV	84.87 \pm 1.02	87.09 \pm 0.93	90.97 \pm 0.43	91.52 \pm 0.44	94.71 \pm 0.31	95.20 \pm 0.28	<u>95.72 \pm 0.10</u>	<u>96.04 \pm 0.10</u>	98.88 \pm 0.08	98.83 \pm 0.08
STRUCTURAL	CORA	58.52 \pm 1.19	63.83 \pm 1.49	67.86 \pm 1.65	70.15 \pm 1.55	<u>85.24 \pm 1.55</u>	87.54 \pm 1.26	85.11 \pm 1.27	<u>87.96 \pm 1.02</u>	94.59 \pm 1.37	93.83 \pm 1.90
	CITSEER	56.39 \pm 1.94	63.32 \pm 1.75	62.93 \pm 2.25	66.21 \pm 1.46	80.07 \pm 1.31	84.06 \pm 1.42	<u>81.53 \pm 1.28</u>	<u>85.00 \pm 1.44</u>	94.05 \pm 0.73	93.25 \pm 0.84
	PUBMED	63.25 \pm 0.37	72.54 \pm 0.30	<u>86.30 \pm 0.55</u>	84.81 \pm 0.29	79.59 \pm 0.75	84.81 \pm 0.47	82.93 \pm 0.41	<u>86.62 \pm 0.37</u>	97.16 \pm 0.24	96.80 \pm 0.30
	OGBN-ARXIV	84.97 \pm 1.02	87.26 \pm 0.87	90.97 \pm 0.43	91.53 \pm 0.43	94.69 \pm 0.29	95.17 \pm 0.25	<u>95.71 \pm 0.09</u>	<u>96.03 \pm 0.10</u>	98.63 \pm 0.13	98.56 \pm 0.13
	SAILING	95.78 \pm 0.20	95.25 \pm 0.24	96.03 \pm 0.20	95.21 \pm 0.32	97.89 \pm 0.12	97.67 \pm 0.17	<u>97.97 \pm 0.08</u>	<u>97.80 \pm 0.09</u>	98.72 \pm 0.18	98.42 \pm 0.28

**Figure 5: Visualization for transductive (Cora) and inductive (Flickr): raw features and features after reconstruction.****Table 5: Ablation studies of the reconstruction and co-label linking on different datasets.**

	Cora	Pubmed	Flickr	Reddit
w/o Rec	78.64 \pm 1.14	77.74 \pm 0.67	50.83 \pm 0.16	92.68 \pm 0.04
w/o CLL	77.10 \pm 1.02	77.98 \pm 0.59	51.93 \pm 0.11	93.96 \pm 0.07
w/ Rec and CLL	79.62 \pm 0.39	78.56 \pm 0.56	51.97 \pm 0.07	93.95 \pm 0.15

feature completion previously handled by FP. We also visualize the Flickr dataset under the inductive setting, as shown in Figure 5. Due to the large number of nodes in the Flickr dataset, we chose the two most common node labels and randomly sampled 3% of them to visualize. We find that after reconstruction, there is better separation between the green and yellow nodes compared to the distribution before reconstruction. This strongly demonstrates that we successfully address the issue of differing feature distributions using a MAE structure, which significantly contributes to solving the problem under the inductive setting.

5 Related Work

Missing node features imputation. Some existing studies [14, 15, 17, 25, 27, 38] explore methods to improve the performance of Graph Neural Networks (GNNs) in handling missing data. SAT [4] introduces a Transformer-like model for feature reconstruction alongside a GNN model to address downstream tasks. GCNMF [27] represents missing data using a Gaussian Mixture Model; however, its performance significantly declines when the proportion of missing features is high. PaGNN [15] proposes two novel partial

aggregation (reconstruction) functions specifically designed for incomplete graphs. Feature Propagation (FP) [25], a general approach for managing missing node features in graph machine learning tasks, includes an initial diffusion-based feature reconstruction step followed by a downstream GNN. ADS-VAE [17] applies VAE model to learn the feature imputation, but it needs excessive space consumption and achieves poor performance on complete datasets with multiple connected components. While these methods have shown promising results in transductive graph learning tasks, they are not well-suited for inductive tasks. Also, they are tailored for fully-connected graphs, which makes their performance seriously decline on graphs with many connected components.

Inductive Learning on graphs. Transductive GNNs are limited to making predictions on nodes and edges seen during training. In contrast, inductive GNNs can generalize to previously unseen nodes and edges, making them more versatile for real-world applications. GraphSAGE [8] generates embeddings by sampling and aggregating features from a node’s local neighborhood, enabling the model to infer embeddings for new nodes that were not present during training. GAT [31] assigns different weights to the neighboring nodes during the aggregation process, allowing the model to focus on the most relevant parts of the graph. Some recent studies have developed inductive GNN models for recommender systems [40, 41]. [39] propose a graph sampling approach to build subgraphs for training GNNs on large graph datasets.

Graph Autoencoders. Autoencoders [11] are designed to reconstruct specific inputs based on the given contexts and do not impose

any decoding order, unlike autoregressive methods. Graph Autoencoders mostly adopt structural and feature reconstruction as their objectives [24, 32]. Masked Autoencoders (MAEs) [9] are a type of neural network architecture primarily designed for self-supervised learning tasks. GraphMAE [12] leverages the inherent structure of graph data to improve learning and representation by masking and predicting parts of the graph during training.

6 Conclusion

In this paper, we introduced DDFI, a novel approach that combines feature propagation and a graph masked autoencoder to effectively impute missing features in both transductive and inductive settings. It leverages a simple yet powerful co-label linking technique to improve the performance of feature propagation. Furthermore, by training a GraphMAE model with diverse views generated through edge dropping, it learns to reconstruct features with robustness and generalization. To evaluate the effectiveness, we conducted extensive experiments on seven datasets, including four public datasets with uniformly missing features and two public datasets with structurally missing features. Additionally, we proposed a novel dataset called Sailing, containing naturally missing features that follows real-world scenarios. The results demonstrate that DDFI outperforms state-of-the-art methods across all datasets and settings, highlighting its effectiveness in attribute graph analysis tasks with missing features.

References

- [1] Danish Maritime Authority. 2023. Historical AIS Data. <http://web.ais.dk/aisdata/>.
- [2] Hongyun Cai, Vincent W Zheng, and Kevin Chen-Chuan Chang. 2018. A comprehensive survey of graph embedding: Problems, techniques, and applications. *IEEE transactions on knowledge and data engineering* 30, 9 (2018), 1616–1637.
- [3] Deli Chen, Yankai Lin, Wei Li, Peng Li, Jie Zhou, and Xu Sun. 2020. Measuring and relieving the over-smoothing problem for graph neural networks from the topological view. In *Proceedings of the AAAI conference on artificial intelligence*, Vol. 34. 3438–3445.
- [4] Xu Chen, Siheng Chen, Jiangchao Yao, Huangjie Zheng, Ya Zhang, and Ivor W Tsang. 2020. Learning on attribute-missing graphs. *IEEE transactions on pattern analysis and machine intelligence* 44, 2 (2020), 740–757.
- [5] Yuchen Fang, Yanjun Qin, Haiyong Luo, Fang Zhao, Bingbing Xu, Liang Zeng, and Chenxing Wang. 2023. When spatio-temporal meet wavelets: Disentangled traffic forecasting via efficient spectral graph attention networks. In *2023 IEEE 39th International Conference on Data Engineering (ICDE)*. IEEE, 517–529.
- [6] Tom Fawcett. 2006. An introduction to ROC analysis. In *Pattern recognition letters*, Vol. 27. Elsevier, 861–874.
- [7] Matthias Fey and Jan Eric Lenssen. 2019. Fast graph representation learning with PyTorch Geometric. In *arXiv e-prints*. <https://arxiv.org/abs/1903.02428>
- [8] Will Hamilton, Zitao Ying, and Jure Leskovec. 2017. Inductive representation learning on large graphs. *Advances in neural information processing systems* 30 (2017).
- [9] Kaiming He, Xinlei Chen, Saining Xie, Yanghao Li, Piotr Dollár, and Ross Girshick. 2022. Masked autoencoders are scalable vision learners. In *Proceedings of the IEEE/CVF conference on computer vision and pattern recognition*. 16000–16009.
- [10] Mikael Henaff, Joan Bruna, and Yann LeCun. 2015. Deep convolutional networks on graph-structured data. *arXiv preprint arXiv:1506.05163* (2015).
- [11] Geoffrey E Hinton and Richard Zemel. 1993. Autoencoders, minimum description length and Helmholtz free energy. *Advances in neural information processing systems* 6 (1993).
- [12] Zhenyu Hou, Xiao Liu, Yukuo Cen, Yuxiao Dong, Hongxia Yang, Chunjie Wang, and Jie Tang. 2022. Graphmae: Self-supervised masked graph autoencoders. In *Proceedings of the 28th ACM SIGKDD Conference on Knowledge Discovery and Data Mining*. 594–604.
- [13] Mengda Huang, Yang Liu, Xiang Ao, Kuan Li, Jianfeng Chi, Jinghua Feng, Hao Yang, and Qing He. 2022. Auc-oriented graph neural network for fraud detection. In *Proceedings of the ACM web conference 2022*. 1311–1321.
- [14] Cuiying Huo, Di Jin, Yawen Li, Dongxiao He, Yu-Bin Yang, and Lingfei Wu. 2023. T2-gnn: Graph neural networks for graphs with incomplete features and structure via teacher-student distillation. In *Proceedings of the AAAI Conference on Artificial Intelligence*, Vol. 37. 4339–4346.
- [15] Bo Jiang and Ziyang Zhang. 2020. Incomplete graph representation and learning via partial graph neural networks. *arXiv preprint arXiv:2003.10130* (2020).
- [16] Bo Jiang, Ziyang Zhang, Doudou Lin, Jin Tang, and Bin Luo. 2019. Semi-supervised learning with graph learning-convolutional networks. In *Proceedings of the IEEE/CVF conference on computer vision and pattern recognition*. 11313–11320.
- [17] Xinke Jiang, Zidi Qin, Jiarong Xu, and Xiang Ao. 2024. Incomplete graph learning via attribute-structure decoupled variational auto-encoder. In *Proceedings of the 17th ACM International Conference on Web Search and Data Mining*. 304–312.
- [18] Thomas N Kipf and Max Welling. 2016. Semi-supervised classification with graph convolutional networks. *arXiv preprint arXiv:1609.02907* (2016).
- [19] Thomas N Kipf and Max Welling. 2016. Variational Graph Auto-Encoders. In *arXiv e-prints*. <https://arxiv.org/abs/1611.07308>
- [20] Thomas N. Kipf and Max Welling. 2017. Semi-Supervised Classification with Graph Convolutional Networks. In *International Conference on Learning Representations*. <https://openreview.net/forum?id=SJU4ayYgl>
- [21] Xin Li, Xiaowen Ying, and Mooi Choo Chuah. 2019. Grip: Graph-based interaction-aware trajectory prediction. In *2019 IEEE Intelligent Transportation Systems Conference (ITSC)*. IEEE, 3960–3966.
- [22] Dongsheng Luo, Tianxiang Zhao, Wei Cheng, Dongkuan Xu, Feng Han, Wenchao Yu, Xiao Liu, Haifeng Chen, and Xiang Zhang. 2024. Towards inductive and efficient explanations for graph neural networks. *IEEE Transactions on Pattern Analysis and Machine Intelligence* 46, 8 (2024), 5245–5259.
- [23] Abdullah Mohamed, Kun Qian, Mohamed Elhoseiny, and Christian Claudel. 2020. Social-scgnn: A social spatio-temporal graph convolutional neural network for human trajectory prediction. In *Proceedings of the IEEE/CVF conference on computer vision and pattern recognition*. 14424–14432.
- [24] Jiwoong Park, Minsik Lee, Hyung Jin Chang, Kyuewang Lee, and Jin Young Choi. 2019. Symmetric graph convolutional autoencoder for unsupervised graph representation learning. In *Proceedings of the IEEE/CVF international conference on computer vision*. 6519–6528.
- [25] Emanuele Rossi, Henry Kenlay, Maria I Gorinova, Benjamin Paul Chamberlain, Xiaowen Dong, and Michael M Bronstein. 2022. On the unreasonable effectiveness of feature propagation in learning on graphs with missing node features. In *Learning on Graphs Conference*. PMLR, 11–1.
- [26] Yifan Song, Darong Lai, Zhihong Chong, and Zeyuan Pan. 2021. Dynamic Network Embedding by Time-Relaxed Temporal Random Walk. In *Neural Information Processing: 28th International Conference, ICONIP 2021, Sanur, Bali, Indonesia, December 8–12, 2021, Proceedings, Part I 28*. Springer, 426–437.
- [27] Hibiki Taguchi, Xin Liu, and Tsuyoshi Murata. 2021. Graph convolutional networks for graphs containing missing features. *Future Generation Computer Systems* 117 (2021), 155–168.
- [28] Daeho Um, Jiwoong Park, Seulki Park, and Jin young Choi. 2023. Confidence-Based Feature Imputation for Graphs with Partially Known Features. In *The Eleventh International Conference on Learning Representations*. <https://openreview.net/forum?id=YPKBilly-Kt>
- [29] Laurens Van der Maaten and Geoffrey Hinton. 2008. Visualizing data using t-SNE. In *Journal of machine learning research*, Vol. 9.
- [30] Petar Veličković, Guillem Cucurull, Arantxa Casanova, Adriana Romero, Pietro Liò, and Yoshua Bengio. 2018. Graph Attention Networks. In *International Conference on Learning Representations*.
- [31] Petar Veličković, Guillem Cucurull, Arantxa Casanova, Adriana Romero, Pietro Lio, Yoshua Bengio, et al. 2017. Graph attention networks. *stat* 1050, 20 (2017), 10–48550.
- [32] Chun Wang, Shirui Pan, Guodong Long, Xingquan Zhu, and Jing Jiang. 2017. Mgae: Marginalized graph autoencoder for graph clustering. In *Proceedings of the 2017 ACM on Conference on Information and Knowledge Management*. 889–898.
- [33] Yiwei Wang, Wei Wang, Yuxuan Liang, Yujun Cai, and Bryan Hooi. 2021. Mixup for node and graph classification. In *Proceedings of the Web Conference 2021*. 3663–3674.
- [34] Yiwei Wang, Wei Wang, Yuxuan Liang, Yujun Cai, Juncheng Liu, and Bryan Hooi. 2020. Nodeaug: Semi-supervised node classification with data augmentation. In *Proceedings of the 26th ACM SIGKDD International Conference on Knowledge Discovery & Data Mining*. 207–217.
- [35] Shunxin Xiao, Shiping Wang, Yuanfei Dai, and Wenzhong Guo. 2022. Graph neural networks in node classification: survey and evaluation. *Machine Vision and Applications* 33, 1 (2022), 4.
- [36] Renchi Yang, Jieming Shi, Keke Huang, and Xiaokui Xiao. 2022. Scalable and effective bipartite network embedding. In *Proceedings of the 2022 International Conference on Management of Data*. 1977–1991.
- [37] Renchi Yang, Jieming Shi, Xiaokui Xiao, Yin Yang, and Sourav S Bhowmick. 2020. Homogeneous network embedding for massive graphs via reweighted personalized pagerank. *Proceedings of the VLDB Endowment* 13, 5 (2020), 670–683.
- [38] Jiaxuan You, Xiaobai Ma, Yi Ding, Mykel J Kochenderfer, and Jure Leskovec. 2020. Handling missing data with graph representation learning. *Advances in Neural Information Processing Systems* 33 (2020), 19075–19087.

- [39] Hanqing Zeng, Hongkuan Zhou, Ajitesh Srivastava, Rajgopal Kannan, and Viktor Prasanna. 2020. GraphSAINT: Graph Sampling Based Inductive Learning Method. In *International Conference on Learning Representations*. <https://openreview.net/forum?id=Bje8pkHFwS>
- [40] Jiani Zhang, Xingjian Shi, Shenglin Zhao, and Irwin King. 2019. STAR-GCN: stacked and reconstructed graph convolutional networks for recommender systems. In *Proceedings of the 28th International Joint Conference on Artificial Intelligence*. 4264–4270.
- [41] Muhan Zhang and Yixin Chen. 2020. Inductive Matrix Completion Based on Graph Neural Networks. In *International Conference on Learning Representations*. <https://openreview.net/forum?id=ByxxgCEYDS>

A Appendix

A.1 Construction of Sailing

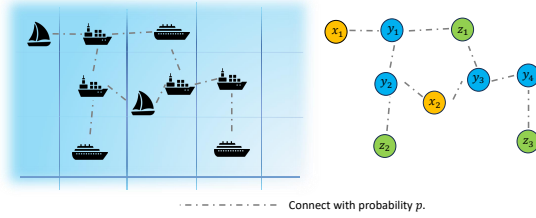


Figure 6: The construction of Sailing dataset.

Our original Sailing dataset contains information about multiple ships, with each ship represented as a node in a graph. The navigation status of each ship serves as a label, with a total of n labels. Edges between nodes are constructed based on the ships' longitude and latitude coordinates. We divide the entire ocean into several small areas using these coordinates. If two nodes are in the same area or in adjacent areas, we create an undirected edge between them with a 50% probability. The process is shown in Figure 6.

The dataset includes both qualitative and quantitative features for each ship. Qualitative features are converted into tensor data using one-hot encoding, while quantitative features are normalized. The Sailing dataset naturally contains missing or invalid data, which we mark as 'NaN'. The statistics of all datasets are listed in Table 1.

A.2 Parameter Settings

For parameter settings, we mainly tune the mask rate and training edge drop rate (we simplify it as drop rate). For the other parameters, we following the setting in GraphMAE. We tune the mask rate in $[0.3, 0.75]$ and training edge drop rate in $[0.1, 0.15]$ for our dataset. The parameters details are shown in Table 6.

Table 6: Parameters for Transductive and Inductive Learning

Parameter	Transductive Learning					Inductive Learning		
	Cora	Citeseer	PubMed	OGBN-Arxiv	Sailing	Flickr	Reddit	Sailing
mask_rate	0.5	0.3	0.75	0.75	0.5	0.5	0.50	0.75
drop_rate	0.1	0.1	0.1	0.1	0.1	0.15	0.1	0.1
encoder	GAT	GCN	GAT	GCN	GAT	GIN	GIN	GIN
decoder	GAT	GCN	GAT	GCN	GAT	GIN	GIN	GIN

A.3 Feature distribution shift validation

According to Section 2.3, the core reason behind the feature distribution shift issue is that the distribution of feature imputed by

Table 7: Δ on Flickr and Reddit.

Dataset	Flickr	Reddit
FP	1.08	0.16
FPMAE	0.86 (\downarrow 20.37%)	0.11 (\downarrow 31.25%)

Table 8: Parameter k 's sensitive analysis for CLL

Dataset	k=5	k=20	k=40
Cora	76.70 \pm 0.72	79.62 \pm 0.39	78.04 \pm 0.19
Pubmed	77.94 \pm 0.43	78.56 \pm 0.56	77.92 \pm 0.44

Table 9: Homogeneity after CLL

Dataset	Cora	Citeseer	PubMed	Ogbn-arxiv
H(G)	0.8252	0.7222	0.7924	0.6358
H(G_con)	0.8317	0.7321	0.7930	0.7776

feature propagation strictly rely on the graph structure, make the difference between training and inference. To validate this, we set the function \mathcal{F} as the Kullback-Leibler Divergence and record the Δ as below. It could be seen that FPMAE can effectively reduce the feature distribution shift.

A.4 Parameter sensitive analysis

We also conduct parameter sensitive analysis on dataset Cora and PubMed with parameter k in CLL. The results are shown below.

From the results in the table, we can get a preliminary conclusion that too small or too large k will have a negative impact on the results. Therefore, we believe that keeping $k = 20$ in the face of different datasets can already achieve excellent results.

A.5 Proof of Improved Homogeneity after CLL

It can be strictly proved that the homogeneity $H(\tilde{G}) \geq H(G)$, where \tilde{G} is the graph enhanced by the CLL algorithm. The equality achieves if and only if the CLL algorithm does not add any edge ($\tilde{G} = G$). For $\forall v_i \in G$, the homophily index of the node $H(v_i) = \frac{N_{L_{v_i}}}{N_{v_i}}$, where $N_{L_{v_i}}$ means the number of neighbors that have the same label with v_i . If the CLL add t edges for v_i , the homophily index will become $H(v_i) = \frac{N_{L_{v_i}} + t}{N_{v_i} + t} > \frac{N_{L_{v_i}}}{N_{v_i}}$. According to the above analysis, CLL will definitely enhance the homogeneity of the graph unless each label contains only one node. We supplement the homophily index on different datasets below.